UDC 621.357.7

Effect of electrodeposition parameters and tungsten content on properties of Ni-Fe-W alloy deposits and its process cost analysis

C. Joseph Kennady [a], A. Leo [b], P. Esther [c]

[a] Department of Chemistry, Karunya Institute of Technology & Sciences, Coimbatore-641114, India

[b] Department of Commerce and International Trade, Karunya Institute of Technology & Sciences, Coimbatore-641114, India

[c] Department of Physics, LRG Government Arts College for Women, Tirupur-641604, India

Electrodeposition of Ni-Fe-W alloy was carried out from a plating bath containing nickel sulfate, ferrous sulfate, sodium tungstate, boric acid, diammonium citrate and citric acid. Films were electrodeposited at varying pH from 3 to 10 and current density from 1.0 to 6.0 A dm^{-2}. Only the concentration of sodium tungstate in the bath was varied to study the effect of tungsten content on the composition of alloy deposits. Adhesion of the deposit was tested by bend and tape tests. The structure and surface morphology of Ni-Fe-W alloy deposits were examined by XRD and SEM analyses, respectively. The composition of the alloy was determined using EDAX analyzer. A forecast cost analysis was carried out to evaluate the commercial aspect of this process.

Keywords: electrodeposition, Ni-Fe-W alloy deposits, ammoniacal citrate bath, structure, surface morphology, process cost analysis.

DOI: 10.32434/0321-4095-2022-141-2-17-23

Introduction

Electrodeposited alloys of iron group metals have been widely applied in industry, mainly as the materials for magnetic storage devices and electronics [1]. Ni-Fe alloys with varying content of nickel and iron have numerous technological applications due to their excellent properties such as low coefficient of thermal expansion and soft magnetic properties [2]. These alloys are used in glass sealing, thermostatic bimetals, integrated circuit packaging and cathode ray tube shadow mask. Based on their soft magnetic properties, they are widely used on read-write heads for magnetic storage, magnetic actuators, magnetic shielding, and high-performance transformer cores [3].

Many bath compositions were tried with chloride [4–6], sulphate [7], fluoborate [8,9] and sulphamate [10–12] salts for the electrodeposition of Ni-Fe alloy with desired properties. All these baths were encountered some shortcomings such as requirement of high temperature, high current density, high cost, corrosivity, wastewater treatment cost and harmful byproducts. To avoid precipitation of Fe, baths were prepared with complexing agents such as citric acid [13].

The introduction of tungsten to binary Ni-Fe alloy improved the durability, corrosion resistance and thermal stability [14]. Corrosion properties of electrodeposited Ni-W alloy deposits were studied using inhibitors [15]. Very few papers [16,17] reported the electrodeposition of ternary tungsten alloys and discussed corrosion behavior and steel part coverings. In the present work, the effect of sodium tungstate on the tungsten content of the deposit and the structure and surface morphology of the deposits was studied. The electrodeposition of crystalline Ni-Fe-W alloy films was done in this work from a citrate based and environmentally friendly plating solution.

Experimental

A copper substrate of 4.0×1.0 cm was used as cathode and a stainless steel of the same size was used as anode for galvanostatic electrodeposition experiments. Required current for the electrodeposition was passed from a regulated direct current power supply. Electrodeposition of alloys was carried out with varying current densities. The copper substrate was degreased and slightly activated with 5% sulfuric acid just before electrodeposition. Thin micrometer-thick films of Ni-Fe-W alloy were electrodeposited from a plating bath solution, containing nickel sulfate (60 g l^{-1}),

ferrous sulfate ($FeSO_4 \cdot 7H_2O$) (30 g l^{-1}), sodium tungstate (5–10 g l^{-1}), boric acid (10 g l^{-1}), diammonium citrate (70 g l^{-1}) and citric acid (5 g l^{-1}). Deposition time was fixed at 30 min and temperature at 75^0C, which resulted in 5–20 μm thick layers. pH of the bath was varied by appropriate addition of ammonia solution. Adhesion of the deposits were tested bend test by bending the sample for 360^0.

After electrodeposition the composition of Ni-Fe-W alloy deposit was determined using a JEOL 6390 Scanning Electron Microscope SEM) with an EDX analyzer. The microstructure of the deposit was tested by Shimadzu X-ray diffractometer (XRD) employing Cu target K_α radiation.

Results and discussion

Electrodeposition

The as-deposited samples were tested for its surface appearance and were found bright and uniform in appearance. The deposits were not peeled off from the substrate during the bend test.

Effect of pH

The Ni-Fe-W alloy can be deposited from the citrate bath in a relatively wide range of pH. At low values (pH<5), polytungstate is formed followed by the precipitation of tungstic acid. At pH>10, iron hydroxide is formed. The pH range suitable for the electrodeposition of alloy layers is 5–10. The compositions of the alloys deposited at various pH ranges are shown in Fig. 1. As pH increases, tungsten and nickel contents increase, but iron content decreases. A decrease in iron content is due to its precipitation. Higher tungsten content was obtained at pH 8.

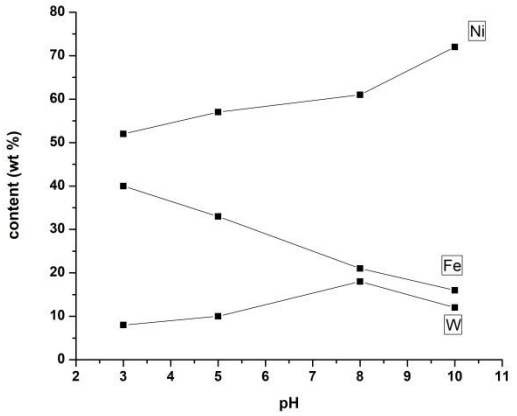

Fig. 1. Composition of Ni-Fe-W alloy deposit electrodeposited at various pH at the current density of 4 A dm^{-2} and temperature of 75^0C

Effect of current density

Figure 2 shows the composition of ternary Ni-Fe-W alloys as a function of current density. The nickel content decreases with increasing current density. However, the iron content remains almost the same. At the same time, the tungsten content increases in conjunction with a decrease of nickel content. Films deposited at current densities more than 3 A dm^{-2} have weaker adhesion to the substrate.

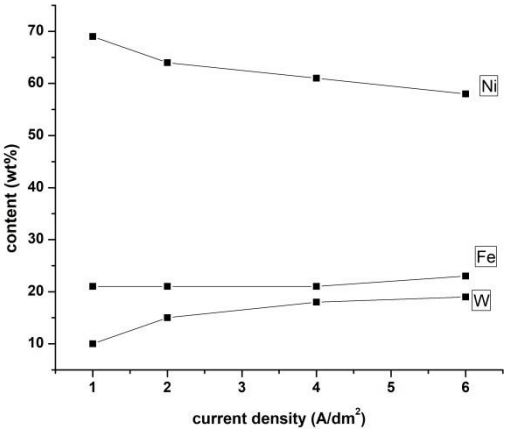

Fig. 2. Composition of Ni-Fe-W alloy deposit electrodeposited at various current density at the pH value of 8 and temperature of 75^0C

Effect of sodium tungstate

Figure 3 shows the composition of ternary Ni-Fe-W alloys as a function of concentration of sodium tungstate. The tungsten content increases in conjunction with a decrease of nickel content and then almost remains the same as the concentration of sodium tungstate increases. At the concentration of 10 g l^{-1}, the tungsten content is high as 14.3 wt.%.

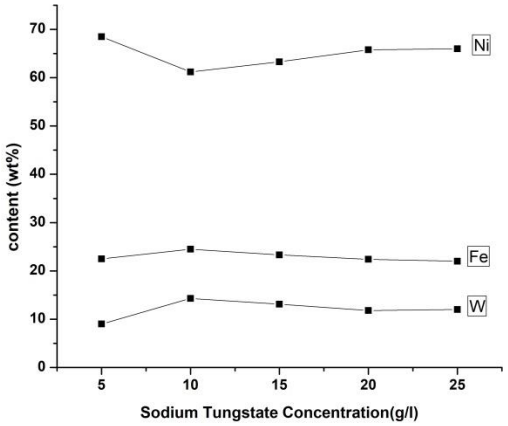

Fig. 3. Composition of Ni-Fe-W alloy deposit electrodeposited at 1 A dm^{-2} at various concentration of sodium tungstate at the pH value of 8 and temperature of 75^0C

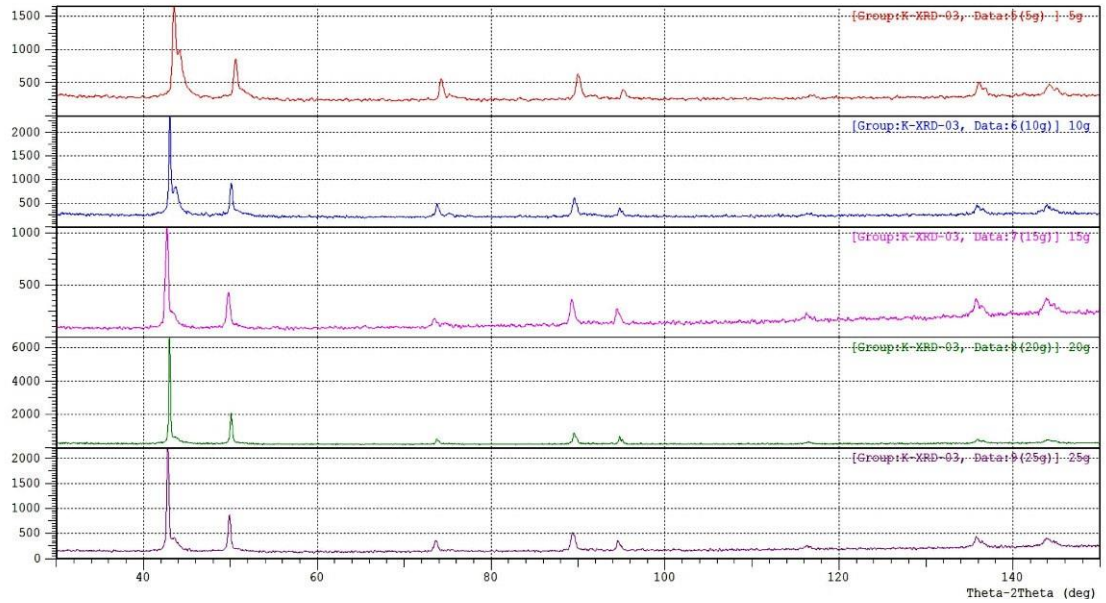

Fig. 4. X-ray diffraction pattern for Ni-Fe-W deposited at varying concentration of sodium tungstate (top to bottom: 5 g l^{-1}, 10 g l^{-1}, 15 g l^{-1}, 20 g l^{-1}, and 25 g l^{-1}). pH 8; current density 1 A dm^{-2}

Microstructure and surface morphology of electrodeposited alloys

The structure of the alloy films electrodeposited at current density of 1 A dm^{-2} for various concentration of sodium tungstate was determined by XRD analysis (Fig. 4). For ternary alloys when the tungsten content is low (<25 wt.%), the structure of deposits is crystalline**.** It can be concluded that the alloy deposits show diffraction peaks of FeNi (111), Ni_4W (211), Fe_7W_6 (116), and Fe_6W_6C phases. The apparent grain sizes were calculated using the Scherer formula:

$$Dhkl=K\lambda/\beta\cdot\cos\theta,$$

where K is the Scherer constant with the value of 0.94, λ is the X-ray wavelength (0.15406 nm) for Cu target, θ is the Bragg angle and β is the peak half width in radian unit.

XRD patterns of the deposit show crystalline structure for various sodium tungstate concentrations. The sharp peak at $2\theta=43.315^0$ and $\beta=0.9^0$ was used to calculate the grain size of the alloy deposited at pH 8, and the grain size was found to be 10 nm which is in nanoscale.

At low current density and low pH as seen in Fig. 5,a, the surface is bright and rough with some cracks due to internal stress. At low pH and high current density as in Fig. 5,b, the surface is uniform with cracks due to internal stress. Alloy deposited at high pH and high current density has uniform granular structure on the smooth surface.

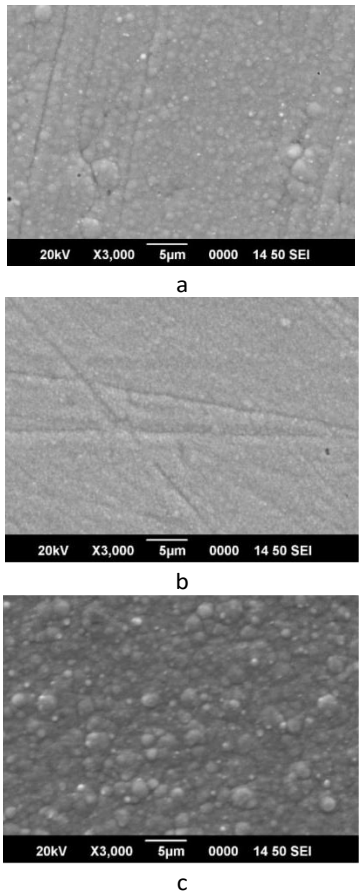

Fig. 5. SEM images of alloys coatings deposited fat different pH and current density combinations: a – pH 3 and current density 1 A dm^{-2}, b – pH 3 and current density 4 A dm^{-2} and c – pH 8 and current density 4 A dm^{-2}

Process cost analysis

Following chemicals (Fig. 6) are used in the research and the economic viability of the process is determined through the basic cost determination techniques. The techniques used are process cost analysis and forecast cost analysis.

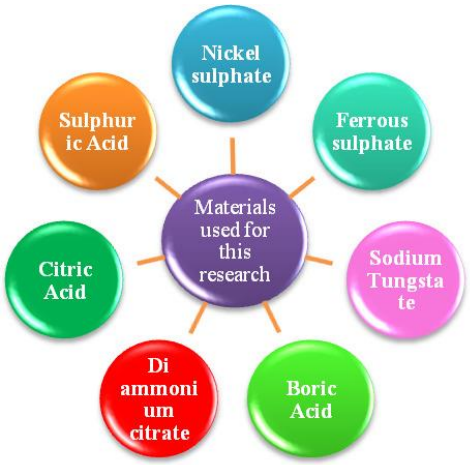

Fig. 6. Chemicals used for the electrodeposition of Ni-Fe-W alloy

Tables 1 and 2 contain expenses related to materials which are used in this research year-wise. The materials used are sulfuric acid (5% of 1000 ml=50 ml), nickel sulfate (60 g l^{-1}), ferrous sulfate (30 g l^{-1}), sodium tungstate (10 g l^{-1}), boric acid (10 g l^{-1}), diammonium citrate (70 g l^{-1}), and citric acid (5 g l^{-1}). The expenses divided from Table 2 for bulk purchased materials. It shows that the amount spent was 23.87$, 25.02$, 28.47$, 31.24$, and 33.01$ in 2017, 2018, 2019, 2020, and 2021, respectively. Through these Tables, it is concluded that the cost of the research is economically suitable.

Table 3 contains forecast analysis of expenses related to materials on the same basis as above, which are used in this research for the upcoming years. The expenses taken from the process cost analysis table and the total expenses determined up to 2026. Forecast analysis has done through MS-Excel (https://www.ablebits.com/office-addins-blog/2019/03/13/excel-forecast-function-formula-examples/).

The FORECAST function predicts a value based on existing values along a linear trend (Fig. 7). FORECAST function calculation can be used for future value predictions using linear regression;

Table 1. Cost analysis for purchased materials in US dollars

S. No.	Year	Sulfuric acid (1 liter)	Nickel sulfate (500 g)	Ferrous sulfate (500 g)	Sodium tungstate (454 g)	Boric acid (1 liter)	Diammonium citrate (454 g)	Citric acid (2.9 Liter)	Total
1	2017	38.37	15.32	116.55	36.59	60.94	74.81	101.33	443.92
2	2018	42.40	16.26	122.47	39.70	64.03	77.68	106.31	468.85
3	2019	51.87	16.80	133.71	51.23	75.55	89.23	113.82	532.22
4	2020	58.32	18.28	146.08	62.99	90.31	96.49	118.93	591.39
5	2021	63.52	20.16	151.05	79.44	95.09	100.18	121.10	630.54

Table 2. Process cost (in US dollars) analysis of materials consumed in this research

S. No.	Year	Sulfuric acid (5% of 1000 ml=50 ml)	Nickel sulfate (60 g)	Ferrous sulfate (30 g)	Sodium tungstate (10 g)	Boric acid (10 ml)	Diammonium citrate (70 g)	Citric acid (5 ml)	Total
1	2017	1.92	1.84	6.99	0.81	0.61	11.53	0.17	23.87
2	2018	2.12	1.95	7.35	0.81	0.65	11.98	0.18	25.03
3	2019	2.59	2.02	8.02	1.13	0.76	13.76	0.20	28.47
4	2020	2.92	2.19	8.76	1.39	0.90	14.88	0.20	31.25
5	2021	3.18	2.42	9.06	1.75	0.95	15.45	0.21	33.01

Table 3. Forecast cost (in US dollars) analysis for upcoming years

S. No.	Years	Sulfuric acid (5% of 1000 ml=50 ml)	Nickel sulfate (60 g)	Ferrous sulfate (30 g)	Sodium tungstate (10 g)	Boric acid (10 ml)	Diammonium citrate (70 g)	Citric acid (5 ml)	Total
1	2022	3.54	2.50	9.71	1.92	1.06	16.74	0.22	35.67
2	2023	3.87	2.64	10.26	2.16	1.15	17.81	0.23	38.12
3	2024	4.20	2.78	10.82	2.41	1.24	18.88	0.24	40.57
4	2025	4.53	2.93	11.37	2.66	1.34	19.95	0.25	43.02
5	2026	4.86	3.07	11.93	2.90	1.43	21.02	0.26	45.47

predict numeric values like sales, inventory, test scores, expenses, measurements, etc. It shows that the cost will be 33.76$, 38.12$, 40.57$, 43.02$, and 45.47$ in 2022, 2023, 2024, 2025, and 2026, respectively.

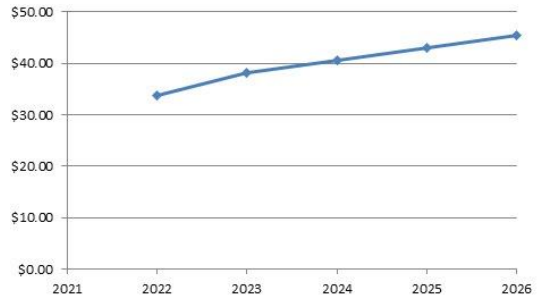

Fig. 7. Forecast cost analysis for upcoming years for the electrodeposition of Ni-Fe-W alloy coatings

Conclusions

Ni-Fe-W alloy deposits were obtained from ammoniacal citrate bath by electrodeposition process. The effect of pH and current density on the tungsten content and properties were studied. As the current density increases, tungsten content in the alloy increases. As pH increases, tungsten content increases to a maximum value at pH 8 and then decreases at pH 10. XRD patterns revealed the presence of various phases Ni_4W, FeNi, Fe_6W_6C and Fe_7W_6 in the deposits. The deposits are uniform and nanocrystalline, they have a granular surface morphology. The deposit obtained at pH 8 and current density 4 A dm^{-2} is found to be smooth and have no cracks. This Ni-Fe-W alloy deposit (61Ni-21Fe-18W) electrodeposited from the citrate bath can be further studied with respect to electrical, magnetic and corrosion properties. Process and forecast cost analysis supports this process of electrodeposition on account of economic feasibility.

References

1. *Alloy* electrodeposition for electronic applications / Cavalotti P.L., Bozzini B., Nobili L., Zangari G. // Electrochim Acta. – 1994. – Vol.39. – P.1123-1131.
2. *Electrodeposition* of Ni-Fe alloys, composites, and nano coatings – a review / Torabinejad V., Aliofkhazraei M., Assareh S., Allahyarzadeh M.H., Rouhaghdam A.S. // J. Alloys Compd. – 2017. – Vol.691. – P.841-859.
3. *Properties* and applications for electrodeposited nanocrystalline Fe-Ni alloys / McCrea J.L., Palumbo G., Hibbard G.D., Erb U. // Rev. Adv. Mater. Sci. – 2003. – Vol.5. – No. 3. – P.252-258.
4. *Harty S.F., McGeough J.A., Tulloch R.M.* A review of the electroforming of iron and iron-nickel alloy // Surf. Technol. – 1981. – Vol.12. – P.39-55.
5. *Gadad S., Harris T.M.* Oxygen incorporation during the electrodeposition of Ni, Fe, and Ni-Fe alloys // J. Electrochem. Soc. – 1998. – Vol.145. – P.3699-3703.
6. *Kieling V.C.* Parameters influencing the electro-deposition of Ni-Fe alloys // Surf. Coat. Technol. – 1997. – Vol.96. – P.135-139.
7. *Nagayama T., Yamamoto T., Nakamura T.* Thermal expansions and mechanical properties of electrodeposited Fe–Ni alloys in the Invar composition range // Electrochim. Acta. – 2016. – Vol.205. – P.178-187.
8. *Electrodeposition* of Ni, Fe and Ni–Fe alloy on a 316 stainless steel surface in a fluorborate bath / Su C.W., He F.J., Ju H., Zhang Y.B., Wang E.L. // Electrochim. Acta. – 2009. – Vol.54. – P.6257-6263.
9. $Ni_{1-x}Fe_x$ ($0.1 < x < 0.75$) alloy foils prepared from a fluorborate bath using electrochemical deposition / Su C.W., Wang E.L., Zhang Y.B., He F.J. // J. Alloys Compd. – 2009. – Vol.474. – P.190-194.

10. *Grimmett D.L., Schwartz M., Nobe K*. Pulsed electrodeposition of iron-nickel alloys // J. Electrochem. Soc. – 1990. – Vol.137. – P.3414-3418.
11. *Trudeau M.L*. Nanocrystalline Fe and Fe-riched Fe-Ni through electrodeposition // Nanostruct. Mater. – 1999. – Vol.12. – P.55-60.
12. *Dubin V.M., Lisunova M.O., Walton B.L*. Invar electrodeposition for controlled expansion interconnects // J. Electrochem. Soc. – 2017. – Vol.164. – P.D321-D326.
13. *Brankovic S.R., Bae S.E., Litvinov D*. The effect of Fe^{3+} on magnetic moment of electrodeposited CoFe alloys – experimental study and analytical model // Electrochim. Acta. – 2008. – Vol.53. – P.5934-5940.
14. *Donten M., Cesiulis H., Stojek Z*. Electrodeposition and properties of Ni-W, Fe-W and Fe-Ni-W amorphous alloys. A comparative study // Electrochim. Acta. – 2000. – Vol.45. – P.3389-3396.
15. *Influence* of p-hydroxy benzaldehyde on the corrosion properties of Ni–W coating on mild steel / Pramod Kumar U., Saranya S., Parameswari K., Joseph Kennady C. // Voprosy Khimii i Khimicheskoi Tekhnologii. – 2017. – No. 5. – P.11-18.
16. *Sriraman K.R., Raman S.G.S., Seshadri S.K*. Corrosion behaviour of electrodeposited nanocrystalline Ni–W and Ni–Fe–W alloys // Mater. Sci. Eng. A. – 2007. – Vol.460-461. – P.39-45.
17. *Castelli C.Z., Neto A.F.A*. Development of Fe-Ni-W alloys for steel parts coverings // Chem. Eng. Trans. – 2019. – Vol.74. P.1189-1194.

Received 27.09.2021

Вплив параметрів електроосадження та вмісту вольфраму на властивості гальваноосадів сплавів Ni-Fe-W та аналіз його технологічної вартості

К. Джозеф Кенеді, А. Лео, П. Естер

Електроосадження сплаву Ni-Fe-W проводили з електролітичної ванни, що містить нікель сульфат, залізо сульфат, натрій вольфрамат, борну кислоту, діамоній цитрат та лимонну кислоту. Електроосадження проводили при змінюванні pH від 3 до 10 і густини струму від 1,0 до 6,0 А $дм^{-2}$. Для вивчення впливу вмісту вольфраму в складі покриттів сплавів варіювали лише концентрацію натрій вольфраму у електролітичній ванні. Адгезію осаду перевіряли випробуваннями на згин і методом гнучкої стрічки. Досліджено структуру та поверхневу морфологію осадів сплавів Ni-Fe-W за допомогою методів рентгенівської дифракції та сканівної електронної мікроскопії, відповідно. Склад сплаву визначали за допомогою методу енергодисперсійної рентгенівської спектроскопії. Для оцінки комерційного аспекту цього процесу було проведено аналіз прогнозованих витрат.

Ключові слова: електроосадження; гальваноосади сплавів Ni-Fe-W; аміачно-цитратна електролітична ванна; структура; морфологія поверхні; аналіз витрат.

Effect of electrodeposition parameters and tungsten content on properties of Ni-Fe-W alloy deposits and its process cost analysis

C. Joseph Kennady [a,*], A. Leo [b], P. Esther [c]

[a] Department of Chemistry, Karunya Institute of Technology & Sciences, Coimbatore-641114, India

[b] Department of Commerce and International Trade, Karunya Institute of Technology & Sciences, Coimbatore-641114, India

[c] Department of Physics, LRG Government Arts College for Women, Tirupur-641604, India

[*] e-mail: kennady@karunya.edu

Electrodeposition of Ni-Fe-W alloy was carried out from a plating bath containing nickel sulfate, ferrous sulfate, sodium tungstate, boric acid, diammonium citrate and citric acid. Films were electrodeposited at varying pH from 3 to 10 and current density from 1.0 to 6.0 A dm^{-2}. Only the concentration of sodium tungstate in the bath was varied to study the effect of tungsten content on the composition of alloy deposits. Adhesion of the deposit was tested by bend and tape tests. The structure and surface morphology of Ni-Fe-W alloy deposits were examined by XRD and SEM analyses, respectively. The composition of the alloy was determined using EDAX analyzer. A forecast cost analysis was carried out to evaluate the commercial aspect of this process.

Keywords: electrodeposition; Ni-Fe-W alloy deposits; ammoniacal citrate bath; structure; surface morphology; process cost analysis.

References

1. Cavalotti PL, Bozzini B, Nobili L, Zangari G. Alloy electrodeposition for electronic applications. *Electrochim Acta*. 1994; 39: 1123-1131. doi: 10.1016/0013-4686(94)E0026-V.

2. Torabinejad V, Aliofkhazraei M, Assareh S, Allahyarzadeh MH, Rouhaghdam AS. Electrodeposition of Ni-Fe alloys, composites, and nano coatings – a review. *J Alloys Compd*. 2017; 691: 841-859. doi: 10.1016/j.jallcom.2016.08.329.

3. McCrea JL, Palumbo G, Hibbard GD, Erb U. Properties and applications for electrodeposited nanocrystalline Fe-Ni alloys. *Rev Adv Mater Sci*. 2003; 5(3): 252-258.

4. Harty SF, McGeough JA, Tulloch RM. A review of the electroforming of iron and iron-nickel alloy. *Surf Technol*. 1981; 12: 39-55. doi: 10.1016/0376-4583(81)90135-7.

5. Gadad S, Harris TM. Oxygen incorporation during the electrodeposition of Ni, Fe, and Ni-Fe alloys. *J Electrochem Soc*. 1998; 145: 3699-3703. doi: 10.1149/1.1838861.

6. Kieling VC. Parameters influencing the electrodeposition of Ni-Fe alloys. *Surf Coat Technol*. 1997; 96: 135-139. doi: 10.1016/S0257-8972(97)00078-9.

7. Nagayama T, Yamamoto T, Nakamura T. Thermal expansions and mechanical properties of electrodeposited Fe–Ni alloys in the Invar composition range. *Electrochim Acta*. 2016; 205: 178-187. doi: 10.1016/j.electacta.2016.04.089.

8. Su CW, He FJ, Ju H, Zhang YB, Wang EL. Electrodeposition of Ni, Fe and Ni–Fe alloy on a 316 stainless steel surface in a fluorborate bath. *Electrochim Acta*. 2009; 54: 6257-6263. doi: 10.1016/j.electacta.2009.05.076.

9. Su CW, Wang EL, Zhang YB, He FJ. $Ni_{1-x}Fe_x$ (0.1 < x < 0.75) alloy foils prepared from a fluorborate bath using electrochemical deposition. *J Alloys Compd*. 2009; 474: 190-194. doi: 10.1016/j.jallcom.2008.06.050.

10. Grimmett DL, Schwartz M, Nobe K. Pulsed electrodeposition of iron-nickel alloys. *J Electrochem Soc*. 1990; 137: 3414-3418. doi: 10.1149/1.2086231.

11. Trudeau ML. Nanocrystalline Fe and Fe-riched Fe-Ni through electrodeposition. *Nanostruct Mater*. 1999; 12: 55-60. doi: 10.1016/S0965-9773(99)00065-3.

12. Dubin VM, Lisunova MO, Walton BL. Invar electrodeposition for controlled expansion interconnects. *J Electrochem Soc*. 2017; 164: D321-D326. doi: 10.1149/2.1271706jes.

13. Brankovic SR, Bae SE, Litvinov D. The effect of Fe^{3+} on magnetic moment of electrodeposited CoFe alloys – experimental study and analytical model. *Electrochim Acta*. 2008; 53: 5934-5940. doi: 10.1016/j.electacta.2008.03.071.

14. Donten M, Cesiulis H, Stojek Z. Electrodeposition and properties of Ni-W, Fe-W and Fe-Ni-W amorphous alloys. A comparative study. *Electrochim Acta*. 2000; 45: 3389-3396. doi: 10.1016/S0013-4686(00)00437-0.

15. Pramod Kumar U, Saranya S, Parameswari K, Joseph Kennady C. Influence of p-hydroxy benzaldehyde on the corrosion properties of Ni–W coating on mild steel. *Voprosy Khimii i Khimicheskoi Tekhnologii*. 2017; (5): 11-18.

16. Sriraman KR, Raman SGS, Seshadri SK. Corrosion behaviour of electrodeposited nanocrystalline Ni–W and Ni–Fe–W alloys. *Mater Sci Eng A*. 2007; 460-461: 39-45. doi: 10.1016/j.msea.2007.02.055.

17. Castelli CZ, Neto AFA. Development of Fe-Ni-W alloys for steel parts coverings. *Chem Eng Trans*. 2019; 74: 1189-1194. doi: 10.3303/CET1974199.